

Arrhenius Equation Construction And Nitrate Source Identification Of Denitrification At The Lake Taihu Sediment–Water Interface With ^{15}N Isotope

Qiuxia Ma

Hohai University <https://orcid.org/0000-0002-8362-9319>

Min Pang

Southern University of Science and Technology

Yong Pang (✉ ypang@hhu.edu.cn)

Hohai University

Lu Zhang

Nanjing Institute of Geography and Limnology Chinese Academy of Sciences

Zhilin Huang

Hohai University

Research Article

Keywords: denitrification, Arrhenius equation construction, nitrate source identification, ^{15}N isotope, water temperature

Posted Date: March 18th, 2022

DOI: <https://doi.org/10.21203/rs.3.rs-1453080/v1>

License:  This work is licensed under a Creative Commons Attribution 4.0 International License.

[Read Full License](#)

**Arrhenius equation construction and nitrate source identification of
denitrification at the Lake Taihu sediment–water interface with ¹⁵N isotope**

Qiuxia Ma¹, Min Pang², Yong Pang^{1, *}, Lu Zhang³, Zhilin Huang¹

¹ College of Environment, Hohai University, Nanjing, 210098, China

² School of Environmental Science and Technology, Southern University of Science and Technology,
Shenzhen, 518055, China

³ State Key Laboratory of Lake Science and Environment, Nanjing Institute of Geography and Limnology,
Chinese Academy of Sciences, Nanjing, 210008, China

Corresponding author: Yong Pang Email: ypang@hhu.edu.cn

1 **Abstract:** Total nitrogen in Taihu Lake, China has gradually decreased since 2015 while the total
2 phosphorus concentration has exhibited an increasing trend, indicating an asynchronous change. The
3 dominant nitrogen removal process in freshwater ecosystems is denitrification which primarily occurs at
4 the sediment–water interface. In this study, ¹⁵N isotope incubation experiments were attempted to analyze
5 the effect of water temperature on denitrification, to construct the regional denitrification Arrhenius
6 equations considering water temperature, and to identify the nitrate source of denitrification in Lake
7 Taihu sediments. The results indicated that the potential N₂ production rates and denitrification rates
8 generally decreased in the west to east direction, which was significantly positively correlated with the
9 nitrate concentration of overlying water by Pearson correlation coefficient analysis (P<0.05). In addition,
10 when the water temperature was lower than 30°C, the rates of the potential N₂ production and
11 denitrification were higher with an increase in water temperature, but when the water temperature was
12 overhigh, denitrification was inhibited. The ratio of the total denitrification rate of nitrate from the water
13 column in the sediment to the total denitrification rate during the incubation experiment was above 0.5
14 at each sampling site. This indicated that the denitrification in the Lake Taihu sediment primarily
15 occurred at the expense of nitrate from the water column. Research on denitrification has important
16 implications for improving the water quality of Lake Taihu, and the findings of the study act as a reference
17 for the water environment treatment of other shallow eutrophic lakes in China and globally.

18

19 **Keywords:** denitrification; Arrhenius equation construction; nitrate source identification; ¹⁵N isotope;
20 water temperature

21 1 Introduction

22 Nitrogen enters a lake as inorganic and organic nitrogen through atmospheric deposition, surface
23 runoff, and biological nitrogen fixation, and is absorbed and assimilated by algae, aquatic plants, and
24 benthos (Cottingham et al., 2015; He et al., 2020). These nutrients can be released into the water column
25 through leakage or mortality by organisms (Zhang et al., 2009; Jiang et al., 2019). Human activities have
26 accelerated the input of reactive nitrogen to the biosphere (Frostegard et al., 2021). The increasing input
27 of nitrogen into water is one of the principal anthropogenic stressors leading to lake water eutrophication
28 (Chen et al., 2012; Li et al., 2020).

29 Denitrification, anaerobic ammonium oxidation, and dissimilatory nitrate reduction to ammonium
30 are crucial pathways of dissimilatory nitrate reduction in aquatic ecosystems (Kuypers et al., 2003; Jiang
31 et al., 2019; Jiang et al., 2020; Ahmad et al., 2021). In addition, some researchers have proposed that
32 denitrification is the primary nitrogen removal process in freshwater ecosystems, which occurs at the
33 sediment–water interface (Saunders and Kalff, 2001; Veraart et al., 2011) and is greatly affected by water
34 temperature (Liao et al., 2018; Wang et al., 2018). Additionally, water temperature can directly or
35 indirectly affect denitrification by affecting the dissolved oxygen concentration, nitrogen release, and
36 microbial activity (Gebremariam et al., 2021; Minuti et al., 2021; Wang et al., 2021). Therefore, studies
37 on the effect of denitrification at the sediment–water interface are vital for understanding lake water
38 eutrophication.

39 The most commonly used acetylene inhibition technique is currently considered unsuitable for
40 quantifying the denitrification rates, mainly because of the catalytic decomposition of NO in the presence
41 of acetylene and O₂ (Wu et al., 2019). Nitrogen isotopes have been widely used for understanding

42 inorganic nitrogen sources, migration, and transformation in various environments ((Bu et al., 2017; Jin
43 et al., 2017; Meng et al., 2021). Natural abundance nitrogen ($\delta^{15}\text{N}$) and oxygen isotopes of nitrate ($\delta^{18}\text{O}$)
44 are important tools for evaluating the sources and transformations of natural and contaminant nitrate
45 (NO_3^-) in the environment (Granger and Wankel, 2016). Lewicka–Szczebak et al. (2014) quantified
46 denitrification in arable soils based on stable isotope analyses of emitted N_2O ($\delta^{15}\text{N}$ and $\delta^{18}\text{O}$). Kim et al.
47 (2018) analyzed $\delta^{15}\text{N}$ and $\delta^{18}\text{O}$ using a Finnigan MAT delta plus XL isotope ratio mass spectrometer at
48 the Isotope Science Laboratory to assess denitrification in a hyporheic zone.

49 However, these papers did not propose the relationship between water temperature and
50 denitrification rate, and these methods failed to distinguish the source of substrate nitrate in
51 denitrification.

52 In this study, Lake Taihu in China, a shallow eutrophic lake, was chosen to investigate the effect of
53 water temperature on denitrification at the sediment–water interface with ^{15}N isotope, and the regional
54 denitrification rate equations considering water temperature were established based on the experimental
55 results. The nitrate source of denitrification was identified by direct measurement of the potential N_2
56 production and denitrification rates. Direct measurement of N_2 production has the advantage of
57 quantifying the denitrification rate of using NO_3^- from overlying water and the denitrification rate of
58 using NO_3^- from nitrification within the sediment (Steingruber et al., 2001; Tang et al., 2014).

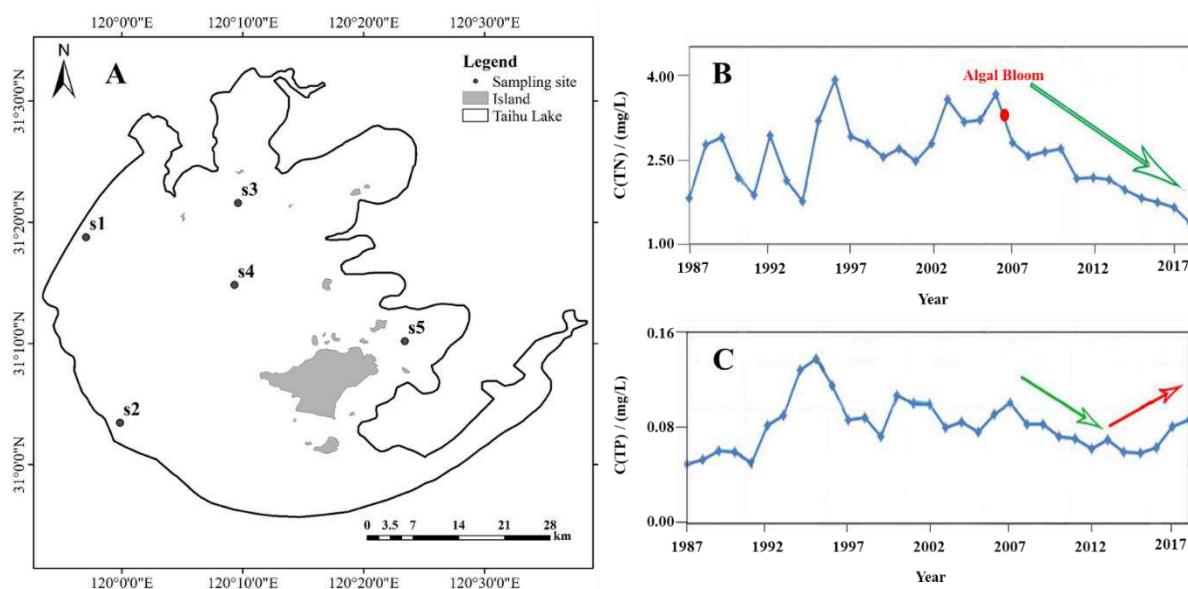
59 **2 Materials and methods**

60 **2.1 Study area description and sample collection**

61 Lake Taihu, located in the eastern plain of China (Jiang et al., 2020), is a large eutrophic shallow

62 (area 2338 km², mean depth 1.9 m) freshwater lake (Zhang et al., 2009). The water temperature ranges
63 from 0°C to 35°C, which is affected by atmospheric temperature (Liu et al., 2015). Lake Taihu has
64 multiple functions, such as flood control, shipping, aquaculture, supporting tourism and recreation,
65 among which the most important function is of water supply (Qin et al., 2015).

66 Samples were collected from five sites referred to as routine monitoring points of the
67 Lake–Watershed Science Sub Center, National Earth System Science Data Center, National Science &
68 Technology Infrastructure of China (<http://gre.geodata.cn>) (Fig. 1A).



69 Fig. 1. Study area and locations of Lake Taihu, China (A), and mean annual concentration of total
70 nitrogen (TN) (B) and total phosphorus (TP) (C) from 1987 to 2018.

71 2.2 Chemical analysis

72 For the lake water quality observation, electrical conductivity, pH, dissolved oxygen, and water
73 temperature were measured using a multiparameter water quality analyzer (YSI Professional Plus,
74 6600V2, USA) at the sampling sites. Other factors related to denitrification are the environmental factors
75 including nitrite (NO₂⁻), nitrate (NO₃⁻), and ammonia nitrogen (NH₄⁺). NO₂⁻ was detected by

76 spectrophotometric method, and NO_3^- was measured by ultraviolet spectrophotometry, and NH_4^+ was
77 measured by Nessler's reagent spectrophotometry (Jiang et al., 2019).

78 The sediment water content was calculated by drying the samples at 105°C for 24 h to a constant
79 weight. The dried samples were burnt at 550°C for 6 h in a muffle furnace to measure the loss on ignition.

80 **2.3 Incubation experiment**

81 The intact sediment cores were placed vertically in the laboratory, and the lake water was filled with
82 a syringe along the pipe wall, by to ensure that the samples were least disturbed. The samples were
83 divided into three groups and incubated in a constant temperature incubator at the 25°C , 30°C , and 35°C
84 for 24 h (Liu et al., 2015). To avoid the influence of algal photosynthesis in the sediment and the water
85 on denitrification, the column samples were wrapped with aluminum foil during cultivation. The
86 sediment cores were incubated in the denitrification incubation system, that included five buckets filled
87 with filtered lake water, a peristaltic pump with constant water flow, sealed pistons, inlet pipes, and outlet
88 pipes. The inlet pipe had to be controlled to be lower than the outlet pipe and maintained approximately
89 1 cm away from the sediment. The filtered lake water was pumped into the sediment cores by a peristaltic
90 pump at a flow rate of 0.78 mL/min, ensuring the overlying water was fully mixed.

91 After the pre-culture experiment, $^{15}\text{NO}_3^-$ was added to each bucket to achieve a final concentration
92 of 100 $\mu\text{mol/L}$, and then steadily incubated at three temperatures for another 24 h (Veraart et al., 2011).
93 The inlet water of each sampling site was carefully collected into the Labco bottles without bubbles using
94 syringes, and the outlet water directly overflowed into the Labco bottles. Following this, 0.2 mL 50%
95 ZnCl_2 was added to each Labco bottle. Eventually, the content of soluble gas ($^{28}\text{N}_2$, $^{28}\text{N}_2$, and $^{30}\text{N}_2$) in the
96 water sample was determined using a membrane interface mass spectrometer (MIMS). In addition, 25

97 mL of inlet and outlet water samples were collected and filtered through 0.45 μm cellulose acetate
 98 membranes to determine the concentration of NO_3^- .

99 2.4 Calculation method of potential N_2 production and denitrification rates

100 Denitrification in the sediment can occur at the expense of NO_3^- from the water column or from
 101 NO_3^- produced within the sediment by nitrification (Steingruber et al., 2001). The main pathway can be
 102 identified using the $^{15}\text{NO}_3^-$ isotope pairing technique (Fig. 2). The dissolved gases used to calculate the
 103 denitrification rates were $^{29}\text{N}_2$ and $^{30}\text{N}_2$, and their corresponding potential production rates r_{29} and r_{30}
 104 were calculated as follows (Tang et al., 2014; Jiang et al., 2020):

$$r_i = \frac{(C_i - C_{i0}) \cdot v}{A} \times 60, \quad (1)$$

105 where r_i ($\mu\text{mol} \cdot \text{m}^{-2} \cdot \text{h}^{-1}$) is the release rate of $^i\text{N}_2$ ($i=29, 30$), C_i , C_{i0} ($\mu\text{mol} \cdot \text{L}^{-1}$) are the
 106 concentrations of $^i\text{N}_2$ in the inlet and outlet water, respectively, v ($\text{mL} \cdot \text{min}^{-1}$) is the flow rate of the
 107 peristaltic pump, A (m^2) is the surface of the incubated sediment, and the time conversion factor is
 108 60.

109 The denitrification rates of $^{15}\text{NO}_3^-$ (D_{15}) and unlabeled $^{14}\text{NO}_3^-$ (D_{14}) can be calculated by the
 110 production rate of $^{29}\text{N}_2$ (r_{29}) and $^{30}\text{N}_2$ (r_{30}), it can normally be expressed as (Steingruber et al., 2001):

$$D_{15} = r_{29} + 2 \cdot r_{30}, \quad (2)$$

$$D_{14} = D_{15} \times \frac{r_{29}}{2 \cdot r_{30}}, \quad (3)$$

111 The total denitrification rate during the incubation experiment (D_{tot}) and the total denitrification rate
 112 of nitrate from the water column (D_{wtot}) were determined by the following equations:

$$D_{\text{tot}} = D_{14} + D_{15}, \text{ and} \quad (4)$$

$$D_{wtot} = D_{15} / \varepsilon, \quad (5)$$

113 where ε is the $^{15}\text{NO}_3^-$ abundance during the incubation and is calculated by the following equation:

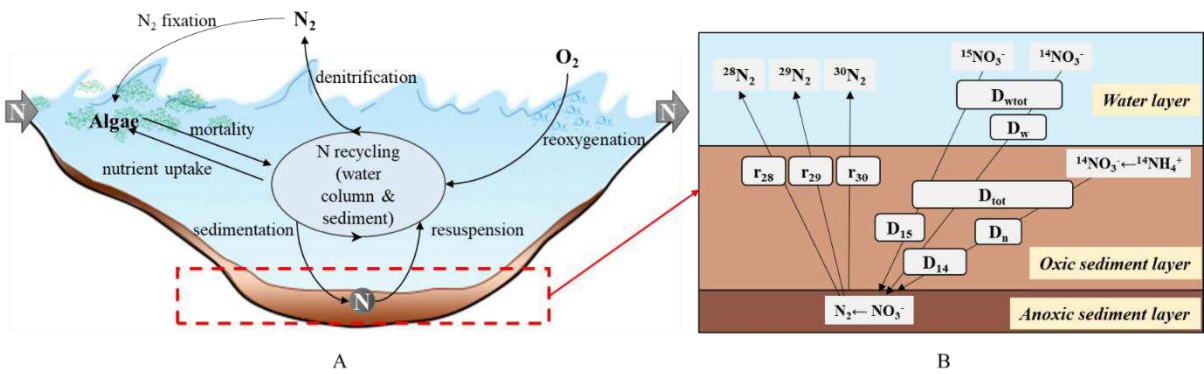
$$\varepsilon = \frac{[\text{NO}_3^-]_a - [\text{NO}_3^-]_b}{[\text{NO}_3^-]_a}, \quad (6)$$

114 where $[\text{NO}_3^-]_a$ and $[\text{NO}_3^-]_b$ are the concentrations referred to after and before the addition of

115 $^{15}\text{NO}_3^-$ tracer addition, respectively.

116 The nitrate source can be identified by the ratio of D_{wtot} to D_{tot} (γ):

$$\gamma = \frac{D_{wtot}}{D_{tot}}, \quad (7)$$



117 Fig. 2. Schematic representation of the nitrogen cycle (A) and the transformation rates during a $^{15}\text{NO}_3^-$

118 tracer experiment (B) in shallow lakes (Steingruber et al., 2001; Qin et al., 2020). r_{28} , r_{29} , and r_{30} are the

119 release rates of $^{28}\text{N}_2$, $^{29}\text{N}_2$, and $^{30}\text{N}_2$, respectively. D_{wtot} is the total uncoupled denitrification rate using

120 nitrate from the water column. D_w refers to the denitrification rate of nitrate from the water column

121 without tracer addition. D_n is the coupled denitrification rate using nitrate from the sediment. D_{15} and

122 D_{14} are the denitrification rates of $^{15}\text{NO}_3^-$ and $^{14}\text{NO}_3^-$, respectively. D_{tot} is the total denitrification

123 during the incubation experiment.

124 3 Results and discussion

125 3.1 Basic physicochemical parameters of the lake water and sediment

126 The basic physicochemical parameters of the lake water and sediment at the sampling sites are
127 shown in Table 1. As for the lake water observation, the pH and water temperature of the five sampling
128 sites were approximately 8 and 25°C, respectively. The dissolved oxygen of s1, and s2 was higher than
129 that of s3, s4, and s5, but the electrical conductivity was evidently lower than that of s3, s4, and s5. In
130 terms of sediment, the average sediment water content of s1, and s2 was nearly 64.35%, and that of the
131 s3, s4, and s5 was approximately 50.24%. The difference in the sediment water content was not
132 significant. However, the loss on ignition of s3, s4, and s5 was approximately eight times that of s1, and
133 s2 because of the presence of more aquatic plants in the east of Lake Taihu (Ticha et al., 2019).

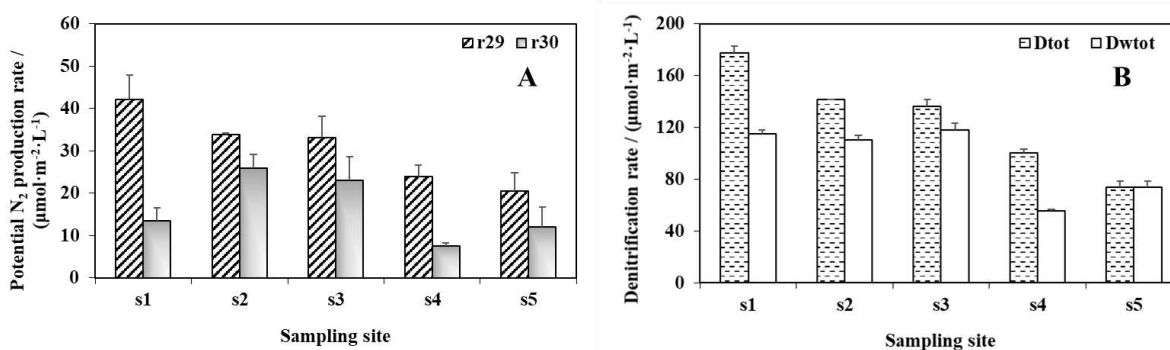
134 **Table 1**

135 Mean values of basic physicochemical parameters of lake water and sediment (the basic physicochemical
136 parameters of lake water were measured at the sampling sites and those of sediment were determined in
137 laboratory; all samples, $n=3$).

Site	Lake water			Sediment		
	pH	Water temperature (°C)	Dissolved oxygen (mg·L ⁻¹)	Electrical conductivity (ms·cm ⁻¹)	Water content (%)	Loss on ignition (%)
s1	7.55	24.5	8.59	0.30	61.72	1.76
s2	7.79	24.9	9.07	0.37	66.97	1.67
s3	8.91	25.6	7.39	0.59	49.30	14.88
s4	8.46	25.1	6.39	0.59	58.32	10.17
s5	8.58	25.0	7.09	0.52	43.09	16.32

138 **3.2 Denitrification rates and construction of Arrhenius equation**

139 The potential N_2 production and denitrification rates of the five sites at $25^\circ C$ were determined by
 140 ^{15}N isotope incubation experiments with MIMS. The results indicated that the denitrification rate had a
 141 decreasing trend in the west to the east direction in Lake Taihu. The potential $^{29}N_2$ rates were higher than
 142 the $^{30}N_2$ rates at five sites (Fig. 3 A). The r_{29} of site s1 ranked first, r_{29} of s2 and s3 equally ranked second,
 143 and r_{29} of s5 was only half that of s1. The r_{30} of s3 was $23.01 \mu mol \cdot m^{-2} \cdot h^{-1}$, second only to s2, and r_{30} of
 144 s4 was the smallest ($7.54 \mu mol \cdot m^{-2} \cdot h^{-1}$). The order of D_{tot} was the same as that of r_{29} , and the D_{tot} of s1
 145 was $177.39 \mu mol \cdot m^{-2} \cdot h^{-1}$ (Fig. 3 B). Except for s4 and s5, the D_{wtot} of the other sites was more than
 146 $100 \mu mol \cdot m^{-2} \cdot h^{-1}$.

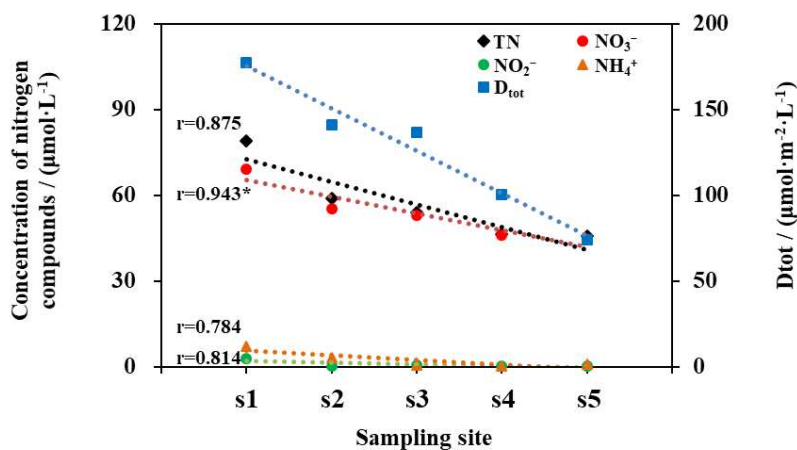


147 Fig. 3. Potential N_2 production (A) and denitrification rates (B) at five sampling sites (water
 148 temperature= $25^\circ C$; all samples, $n=3$). r_{29} and r_{30} are the potential production of $^{29}N_2$ and $^{30}N_2$,
 149 respectively. D_{tot} is the total denitrification during the incubation experiment. D_{wtot} is the total
 150 denitrification rate of nitrate from the water column in the sediment.

151 For the purpose of exploring the reason why the total denitrification rate decreases from west to
 152 East, the concentrations of NO_2^- , NO_3^- , NH_4^+ and TN in the water at each sampling point of Taihu Lake
 153 were detected and analyzed. The concentration of NO_3^- in Lake Taihu was significantly higher than the
 154 concentration of NO_2^- and NH_4^+ (Fig. 4), and showed the same distinct regional differences as D_{tot} ,

155 decreasing from west to east.

156 For further study, the correlation between the total denitrification rate and the concentration of
157 nitrogen compounds in Taihu Lake was analyzed by SPSS statistical software. The statistical results
158 indicated that there was a more significant positive correlation between NO_3^- and D_{tot} (Table 2). And the
159 reason for the spatial distribution of NO_3^- in Taihu Lake is that the western region of Taihu Lake Basin
160 is the main source of pollutants in Taihu Lake, and the eastern region is the drainage area with good water
161 quality (Zhang, 2021).



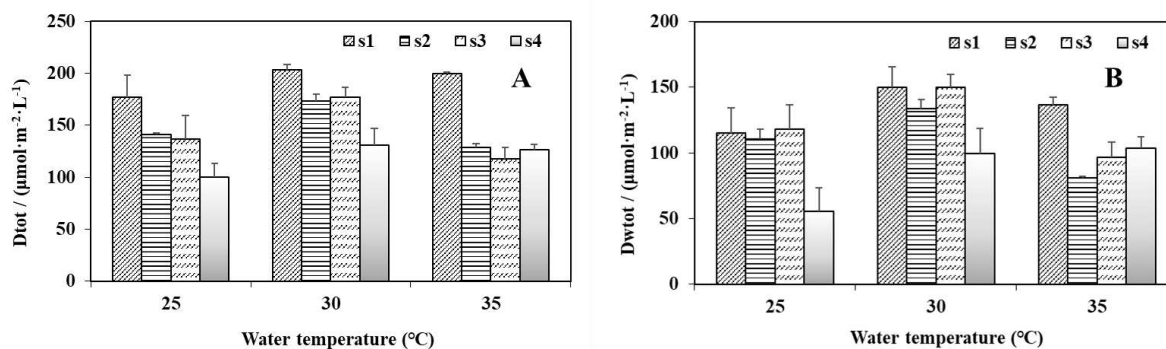
162

163 Fig. 4. Concentration of nitrogen compounds and D_{tot} at the five sampling sites (water
164 temperature=25°C; all samples, $n=3$). r is Pearson correlation coefficient between D_{tot} and nitrogen
165 compound (*. $P<0.05$, significant correlation). D_{tot} is the total denitrification rate during the incubation
166 experiment.

167 In addition, experiments on the effect of water temperature on denitrification were carried out at s1,
168 s2, s3 and s4 points. The results showed that water temperature had a significant effect on denitrification.
169 Specifically, the D_{tot} and D_{wtot} increased with an increase in water temperature when the water
170 temperature ranged from 25°C to 30°C (Fig. 5). The findings of this study were consistent with those of
171 Ma et al. (2008) and Appelboom et al. (2010) on the relationship between water temperature and

172 denitrification. This was mainly due to denitrification reaction could completely take place when the
 173 water temperature was between 10°C and 30°C (Liao et al., 2018), and the increase of water temperature
 174 would reduce the solubility of oxygen in the water under the appropriate water temperature (Veraart et
 175 al., 2011; Zhao et al., 2011) (Table 1). In addition, high temperatures also tended to promote respiration
 176 instead of photosynthesis (Minuti et al., 2021), which further reduces dissolved oxygen. As an anaerobic
 177 reaction, denitrification was enhanced when the concentration of dissolved oxygen in water decreased.

178 High water temperature not only affects the dissolved oxygen in the water column, but also favors
 179 release of nutrients by stimulating microbial mineralization of sediment organic matter, which could
 180 increase pore-water nutrient concentrations, or could erode the oxidized microzone at the
 181 sediment-water interface by increasing oxygen demand (Holdren and Armstrong, 1980; Jiang et al., 2008;
 182 Gebremariam et al., 2021; Wang et al., 2021). Thus, the concentration of the substrate increases and
 183 denitrification is promoted, until the nitrate concentration is saturated (Silvennoinen et al., 2008).



184 Fig. 5. D_{tot} (A) and D_{wtot} (B) rates of s1, s2, s3, and s4 at different water temperatures (all samples,
 185 $n=3$). D_{tot} is the total denitrification during the incubation experiment. D_{wtot} is the total denitrification
 186 rate of nitrate from the water column in the sediment.

187 On the other hand, temperature has a significant influence on the growth of microorganisms (Perez-
 188 Rodriguez et al., 2017). It was obvious from Fig. 5 that when the water temperature exceeded 30°C, the

189 appropriate temperature(Liao et al., 2018), D_{tot} decreased with the increase of water temperature. Through
190 experiments, Wang et al. (2018) found a response to temperature variation, the microorganisms
191 community presented a little difference after a temperature shock, and the N_2 concentration at 34°C was
192 lower than that at 25°C during denitrification. Furthermore, it had been reported that the predominant
193 denitrifying microorganisms belong particularly to the phylum Proteobacteria, when the water
194 temperature was more than 34°C, the activity of the phylum Proteobacteria in Lake Taihu may decrease,
195 resulting in a decrease in the denitrification rates (Xiao et al., 2015; Zhang et al., 2017).

196 Denitrification rate and water temperature conform to Arrhenius equation (Kaspar, 1982; Chi et al.,
197 2004):

$$D_{tot} = D_{tot20^{\circ}\text{C}} \times \theta^{(T-20^{\circ}\text{C})}, \quad (8)$$

198 where $D_{tot20^{\circ}\text{C}}$ ($\mu\text{mol}\cdot\text{m}^{-2}\cdot\text{h}^{-1}$) is the total denitrification rate during the incubation experiment at
199 20°C, θ is the Arrhenius temperature coefficient during denitrification.

200 Based on the experimental results of denitrification rate in Taihu Lake under the condition of
201 sufficient carbon source, the denitrification Arrhenius equation considering the concentration of water
202 temperature can be preliminarily obtained through statistical analysis (Table 2).

203 **Table 2**

204 Denitrification Arrhenius equation for at each sampling site in Taihu Lake.

Sampling site	Denitrification Arrhenius equation
s1	$D_{tot} = 166.01 \times 1.0278^{(T-20^\circ\text{C})}$
s2	$D_{tot} = 128.23 \times 1.0418^{(T-20^\circ\text{C})}$
s3	$D_{tot} = 120.94 \times 1.0532^{(T-20^\circ\text{C})}$
s4	$D_{tot} = 88.75 \times 1.0546^{(T-20^\circ\text{C})}$

205 **3.3 Nitrate source identification of denitrification**

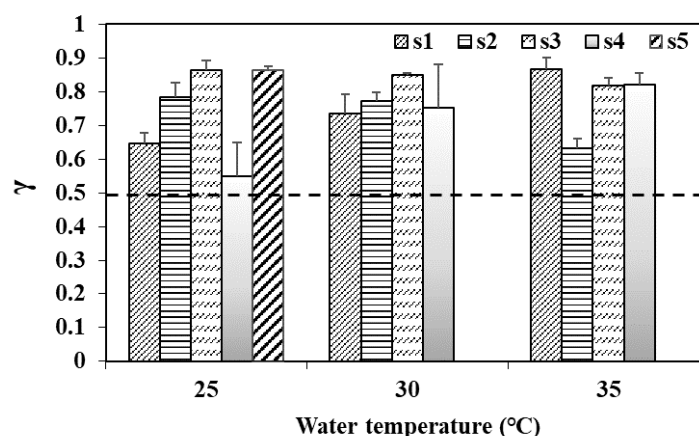
206 As can be seen from Fig. 2 that the total denitrification rate (D_{tot}) was the sum of coupled
 207 denitrification rate rate using nitrate from the water column (D_n) and total uncoupled denitrification rate
 208 using nitrate from the sediment (D_{wtot}) (Svensson et al., 2001). Therefore, the ratio of D_{wtot} to D_{tot} (γ)
 209 can be expressed as:

$$\gamma = \frac{D_{wtot}}{D_{tot}} = \frac{D_{wtot}}{D_{wtot} + D_n}, \quad (9)$$

210 According to formula (9), if $\gamma > 0.5$, it meant that $D_{wtot} > D_n$, which indicates that the nitrate
 211 used for denitrification mainly came from water.

212 Based on D_{wtot} and D_{tot} of each sampling site, the γ was obtained. It was evident that the γ of
 213 the five sampling sites were above 0.5, as illustrated in Fig. 6, which showed that the denitrification at
 214 the Lake Taihu sediment–water interface primarily occurred at the expense of NO_3^- from the water
 215 column. Besides, when the water temperature rose from 25°C to 30°C, the γ increased slightly with
 216 the increase in water temperature, and the increase in s2 and s3 was relatively smaller. When the water

217 temperature approached 35°C, the response γ at each sampling site was inconsistent, but NO_3^- from
 218 the water column was still the main nitrate source of denitrification. In conclusion, the denitrification in
 219 the sediment–water interface mainly occurred at the expense of NO_3^- from the water column, and it was
 220 less affected by water temperature.



221
 222 Fig. 6. Results of the ratios of D_{wtot} to D_{tot} (γ) in incubation experiments at the sites s1, s2, s3, s4, and
 223 s5. D_{tot} is the total denitrification during the incubation experiment. D_{wtot} is the total uncoupled
 224 denitrification rate using nitrate from the water column.

225 3.4 Practical implications of denitrification in shallow eutrophic lakes

226 Due to human activities, such as large-scale synthetic ammonia and large-scale application of
 227 chemical fertilizer, a large amount of exogenous nitrogen enters Taihu Lake, resulting in cyanobacteria
 228 bloom and threatening human drinking water and ecological security (Li et al., 2013). And denitrification
 229 is considered to be the main biological pathway of nitrogen removal, which is of great significance to
 230 reduce Lake nitrogen pollution and eutrophication control (Richardson et al., 2004).

231 Moreover, the algal–bacteria system in the water column can form an important niche that favors
 232 denitrification during cyanobacteria blooms (Chen et al., 2016; Chen et al., 2018). In general, the life of

233 algae is primarily divided into growth and decline periods, and then algae subsides to the bottom of the
234 lake. During the growth period, the oxygen produced by photosynthesis of algae provides an aerobic
235 environment for the nitrifying bacteria attached to the cell mass. This can promote the nitrification of
236 nitrifying bacteria to produce NO_3^- , the substrate for denitrification (Liu et al., 2019). During the decline
237 period, algae are gradually degraded into low molecular weight organic acids (directly available organic
238 carbon) that can be used by denitrifying bacteria (Li et al., 2013).

239 In general, the concentration of TN in water can characterize the effect of nitrogen removal when
240 the external pollution source is certain. From 2003 to 2006, Lake Taihu maintained a high TN
241 concentration, resulting in cyanobacteria blooms in 2007, following which the Cyanobacteria died and
242 were accumulated as sediments. According to the monitoring data, the TN concentration in Lake Taihu
243 gradually decreased from 2008 to 2018 (Fig.1 B). And this further proves that algae contribute to the
244 denitrification during the decay period.

245 Therefore, the study of denitrification in various regions of Taihu Lake can deepen the
246 understanding of nitrogen cycle process in Taihu Lake and contribute to the effective development of
247 water environment and eutrophication control in Taihu Lake.

248 **4 Conclusions**

249 In the present study, the effect of water temperature on denitrification was analyzed by ^{15}N isotope
250 incubation experiments, and the nitrate source of denitrification in Lake Taihu sediment was identified.
251 The results indicated that the denitrification rate showed a decreasing trend in the west to east direction
252 in Lake Taihu. When the water temperature was lower than 30°C , the rates of the potential N_2 production
253 and denitrification were higher with an increase in water temperature, but when the water temperature

254 was overhigh, denitrification was inhibited. And the NO_3^- from the water column was the main nitrate
255 source of denitrification according to the ratio of D_{wtot} to D_{tot} . These findings, and denitrification
256 Arrhenius equations considering water temperature, and further research on denitrification can play an
257 important role in improving the water quality of Lake Taihu, and bear significance for the water
258 environment treatment of other shallow eutrophic lakes in China and globally.

259 **Declaration of Competing Interest**

260 The authors declare that they have no known competing financial interests or personal relationships
261 that could have appeared to influence the work reported in this paper.

262 **Credit Author Statement**

263 Qiuxia Ma: Investigation, Formal analysis, Writing—original draft preparation, Writing—review and
264 editing, Visualization

265 Min Pang: Conceptualization, Methodology, Resources, Supervision

266 Yong Pang: Conceptualization, Resources, Data Curation

267 Lu Zhang: Methodology, Data Curation

268 Zhilin Huang: Investigation, Data Curation

269 **Acknowledgements**

270 This research was supported by the National Natrual Science Foundation of China [Grant Number
271 52000100] and The National Major Science and Technology Project of China [Grant numbers

272 2018ZX07208-005 and 2018ZX07208-007]. We thank the Nanjing Institute of Geography & Limnology
273 Chinese Academy of Sciences for providing the support and help in this experiment.

274 **References**

- 275 Ahmad, H.A., Guo, B.B., Zhuang, X.M., Zhao, Y.Y., S. Ahmad, Lee, T., Zhu, J.G., Dong, Y.L., Ni, S.Q.,
276 2021. A twilight for the complete nitrogen removal via synergistic partial–denitrification, anammox,
277 and DNRA process. *Npj Clean Water* 4(1), 31. <https://doi.org/10.1038/s41545-021-00122-5>.
- 278 Appelboom, T.W., Chescheir, G.M., Birgand, F., Skaggs, R.W., Gilliam, J.W., Amaty, D., 2010.
279 Temperature coefficient for modeling denitrification in surface water sediments using the mass
280 transfer coefficient. *T. Asabe* 53(2), 465–474.
- 281 Bu, X.L., Zhao, C.X., Han, F.Y., Xue, J.H., Wu, Y.B., 2017. Nitrate reduction in groundwater and isotopic
282 investigation of denitrification in integrated tree–grass riparian buffers in Taihu Lake watershed,
283 eastern China. *J. Soil Water Conserv.* 72(1), 45–54. <https://doi.org/10.2489/jswc.72.1.45>.
- 284 Chen, X.C., Huang, Y.Y., Chen, G.Q., Li, P.P., Shen, Y.S., Davis, T.W., 2018. The secretion of organics
285 by living *Microcystis* under the dark/anoxic condition and its enhancing effect on nitrate removal.
286 *Chemosphere* 196, 280–287. <https://doi.org/10.1016/j.chemosphere.2017.12.197>.
- 287 Chen, X.F., Jiang, H.Y., Sun, X., Zhu, Y., Yang, L.Y., 2016. Nitrification and denitrification by
288 algae–attached and free–living microorganisms during a cyanobacterial bloom in Lake Taihu, a
289 shallow Eutrophic Lake in China. *Biogeochemistry* 131(1–2), 135–146.
290 <https://doi.org/10.1007/s10533-016-0271-z>.
- 291 Chen, X.F., Yang, L.Y., Xiao, L., Miao A.J., Xi, B.D., 2012. Nitrogen removal by denitrification during
292 cyanobacterial bloom in Lake Taihu. *J. Freshwater Ecol.* 27(2), 243–258.
293 <https://doi.org/10.1080/02705060.2011.644405>.
- 294 Chi, Y. Z., Li, Y., and Wu, L.P., 2004. Kinetic calculation of pre denitrification biological denitrification

295 process for municipal wastewater. *J. Tianjin Institute of urban construction*. 10(02), 122–124. (In
296 Chinese)

297 Cottingham, K.L., Ewing, H.A., Greer, M.L., Carey, C.C., Weathers, K.C., 2015. Cyanobacteria as
298 biological drivers of lake nitrogen and phosphorus cycling. *Ecosphere* 6(1), 1.
299 <https://doi.org/10.1890/es14-00174.1>.

300 Frostegard, A., Vick, S.H.W., Lim, N.Y.N., Bakken, L.R., Shapleigh, J.P., 2021. Linking meta-omics to
301 the kinetics of denitrification intermediates reveals pH-dependent causes of N₂O emissions and
302 nitrite accumulation in soil. *ISME J.* <https://doi.org/10.1038/s41396-021-01045-2>.

303 Gebremariam, S.Y., McCormick, P., Rochelle, P., 2021. Evidence of a rapid phosphorus-induced regime
304 shift in a large deep reservoir. *Sci. Total Environ.* 782, 146755.
305 <https://doi.org/10.1016/j.scitotenv.2021.146755>.

306 Granger, J., Wankel, S.D., 2016. Isotopic overprinting of nitrification on denitrification as a ubiquitous
307 and unifying feature of environmental nitrogen cycling. *P. Natl. Acad. Sci. USA* 113(42),
308 E6391–E6400. <https://doi.org/10.1073/pnas.1601383113>.

309 He, X.C., Wang, H., Fan, L.L., Liang, D.F., Ao, Y.H., Zhuang, W., 2020. Quantifying physical transport
310 and local proliferation of phytoplankton downstream of an eutrophicated lake. *J. Hydrol.* 585,
311 124796. <https://doi.org/10.1016/j.jhydrol.2020.124796>.

312 Holdren, G.C., Armstrong, D.E., 1980. Factors affecting phosphorus release from intact lake sediment
313 cores. *Environ. Sci. Technol.* 14(1), 79–87.

314 Jiang, X., Jin, X.C., Yao, Y., Li, L.H., Wu, F.C., 2008. Effects of biological activity, light, temperature
315 and oxygen on phosphorus release processes at the sediment and water interface of Taihu Lake,
316 China. *Water Res.* 42(8–9), 2251–2259. <https://doi.org/10.1016/j.watres.2007.12.003>.

- 317 Jiang, X.Y., Gao, G., Zhang, L., Tang, X.M., Shao, K.Q., Hu, Y., 2020. Denitrification and dissimilatory
318 nitrate reduction to ammonium in freshwater lakes of the Eastern Plain, China: Influences of organic
319 carbon and algal bloom. *Sci. Total Environ.* 710, 136303.
320 <https://doi.org/10.1016/j.scitotenv.2019.136303>.
- 321 Jiang, X.Y., Gao, G., Zhang, L., Yao, X.L., Zhao, Z.H., Shen, Q.S., 2019. High rates of ammonium
322 recycling in northwestern Lake Taihu and adjacent rivers: An important pathway of nutrient supply
323 in a water column. *Environ. Pollut.* 252, 1325–1334. <https://doi.org/10.1016/j.envpol.2019.06.026>.
- 324 Jin, Z.F., Gong, J.L., Shi, Y.L., Jin, M.T., Li, F.L., 2017. Nitrate source identification and
325 nitrification–denitrification at the sediment–water interface. *Environ. Sci.* 38(04), 1423–1430. (In
326 Chinese)
- 327 Kim, H., Kaown, D., Mayer, B., Lee, J.Y., Lee, K.K., 2018. Combining pyrosequencing and isotopic
328 approaches to assess denitrification in a hyporheic zone. *Sci. Total Environ.* 631–632, 755–764.
329 <https://doi.org/10.1016/j.scitotenv.2018.03.073>.
- 330 Kaspar, H. F., 1982. Denitrification in marine sediment: measurement of capacity and estimate of in situ
331 rate. *Appl. Environ. Microb.* 43(3), 522–527. <https://doi.org/10.1128/aem.43.3.522-527.1982>.
- 332 Kuypers, M.M.M., Sliemers, A.O., Lavik, G., Schmid, M., Jorgensen, B.B., Kuenen, J.G., Damste, J.S.S.,
333 Strous, M., Jetten, M.S.M., 2003. Anaerobic ammonium oxidation by anammox bacteria in the
334 Black Sea. *Nature* 422(6932), 608–611. <https://doi.org/10.1038/nature01472>.
- 335 Lewicka–Szczepak, D., Well, R., Koster, J.R., Fuss, R., Senbayram, M., Dittert, K., Flessa, H., 2014.
336 Experimental determinations of isotopic fractionation factors associated with N₂O production and
337 reduction during denitrification in soils.
- 338 Li, L.W., Pan, G., Li, L., Li, H., Shi, W.Q., Zhang, H.G., Zhu, G.W., 2013. Effect and mechanism of

339 algae bloom on the denitrification processes in the sediments of Lake Taihu. *J. Lake Sci.* 25(05),
340 628–634. (In Chinese)

341 Li, Y.P., Nwankwegu, A.S., Huang, Y.N., Norgbey, E., Paerl, H.W., Acharya, K., 2020. Evaluating the
342 phytoplankton, nitrate, and ammonium interactions during summer bloom in tributary of a
343 subtropical reservoir. *J. Environ. Manage.* 271, 110971.
344 <https://doi.org/10.1016/j.jenvman.2020.110971>.

345 Liao, R.H., Miao, Y., Li, J., Li, Y., Wang, Z., Du, J., Li, Y.M., Li, A.M., Shen, H.J., 2018. Temperature
346 dependence of denitrification microbial communities and functional genes in an expanded granular
347 sludge bed reactor treating nitrate-rich wastewater. *Rsc Adv.* 8(73), 42087–42094.
348 <https://doi.org/10.1039/c8ra08256a>.

349 Liu, G., Ou, W.X., Zhang, Y.L., Wu, T.F., Zhu, G.W., Shi, K., Qin, B.Q., 2015. Validating and Mapping
350 Surface Water Temperatures in Lake Taihu: Results From MODIS Land Surface Temperature
351 Products. *Ieee J-STARS* 8(3), 1230–1244. <https://doi.org/10.1109/jstars.2014.2386333>.

352 Liu, Z., Xu, H., Zhan, X., Zhu, G., Qin, B., Zhang, Y., 2019. Influence of cyanobacterial blooms on
353 denitrification rate in shallow lake Taihu, China. *Environ. Sci.* 40(03), 1261–1269.
354 <https://doi.org/10.1109/jstars.2014.2386333>. (In Chinese)

355 Ma, J., Peng, Y., Wang, L., Wang, S., 2008. Effect of temperature on denitrification and profiles of pH
356 during the process. *China Environ. Sci.* (11), 1004–1008. (In Chinese)

357 Meng, L.Z., Zhao, Z.L., Lu, L.F., Zhou, J., Luo, D., Fan, R., Li, S.D., Jiang, Q.L., Huang, T., Yang, H.,
358 Huang, C.C., 2021. Source identification of particulate organic carbon using stable isotopes and
359 n-alkanes: modeling and application. *Water Res.* 197, 117083.
360 <https://doi.org/10.1016/j.watres.2021.117083>.

361 Minuti, J.J., Byrne, M., Hemraj, D.A., Russell, B.D., 2021. Capacity of an ecologically key urchin to
362 recover from extreme events: Physiological impacts of heatwaves and the road to recovery. *Sci.*
363 *Total Environ.* 785, 147281. <https://doi.org/10.1016/j.scitotenv.2021.147281>.

364 Perez-Rodríguez, I., Sievert, S.M., Fogel, M.L., Foustoukos, D.I., 2017. Biogeochemical N signatures
365 from rate-yield trade-offs during in vitro chemosynthetic NO₃⁻ reduction by deep-sea vent
366 epsilon-Proteobacteria and Aquificae growing at different temperatures. *Geochim. Cosmochim. Ac.*
367 211, 214–227. <https://doi.org/10.1016/j.gca.2017.05.014>.

368 Qin, B.Q., Li, W., Zhu, G.W., Zhang, Y.L., Wu, T.F., Gao, G., 2015. Cyanobacterial bloom management
369 through integrated monitoring and forecasting in large shallow eutrophic Lake Taihu (China). *J.*
370 *Hazard. Mater.* 287, 356–363. <https://doi.org/10.1016/j.jhazmat.2015.01.047>.

371 Qin, B.Q., Zhou, J., Elser, J.J., Gardner, W.S., Deng, J.M., Brookes, J.D., 2020. Water Depth Underpins
372 the Relative Roles and Fates of Nitrogen and Phosphorus in Lakes. *Environ. Sci. Technol.* 54(6),
373 3191–3198. <https://doi.org/10.1021/acs.est.9b05858>.

374 Richardson, W. B., Strauss, E. A., Bartsch, L. A., Monroe, E. M., Cavanaugh, J. C., Vingum, L., and
375 Soballe, D. M., 2004. Denitrification in the Upper Mississippi River: rates, controls, and
376 contribution to nitrate flux. *Canadian J. Fisheries and Aquatic Sci.* 61(7): 1102-1112.

377 Saunders, D.L., Kalff, J., 2001. Denitrification rates in the sediments of Lake Memphremagog,
378 Canada-USA. *Water Res.* 35(8), 1897–1904. [https://doi.org/10.1016/s0043-1354\(00\)00479-6](https://doi.org/10.1016/s0043-1354(00)00479-6).

379 Silvennoinen, H., Liikanen, A., Torssonen, J., Stange, C.F., Martikainen, P.J., 2008. Denitrification and
380 nitrous oxide effluxes in boreal, eutrophic river sediments under increasing nitrate load: a laboratory
381 microcosm study. *Biogeochemistry* 91(2–3), 105–116. <https://doi.org/10.1007/s10533-008-9262-z>.

382 Steingruber, S.M., Friedrich, J., Gächter, R., Wehrli, B., 2001. Measurement of denitrification in

383 sediments with the N-15 isotope pairing technique. *Appl. Environ. Microb.* 67(9), 3771–3778.
384 <https://doi.org/10.1128/aem.67.9.3771-3778.2001>.

385 Svensson, J. M., Enrich-Prast, A., and Leonardson, L., 2001. Nitrification and denitrification in a
386 eutrophic lake sediment bioturbated by oligochaetes. *Aquat. Microb. Ecol.* 23(2), 177–186.
387 <https://doi.org/10.3354/ame023177>.

388 Tang, C.J., Zhang, L., Du, Y.Y., Yao, X.L., 2014. Spatial variations of denitrification in wetland sediments
389 in Poyang Lake and the influencing factors. *Acta Scientiae Circumstantiae* 34(01), 202–209. (In
390 Chinese)

391 Ticha, A., Besta, T., Vondrak, D., Houfkova, P., Jankovska, V., 2019. Nutrient availability affected
392 shallow-lake ecosystem response along the Late-Glacial/Holocene transition. *Hydrobiologia*
393 846(1), 87–108. <https://doi.org/10.1007/s10750-019-04054-7>.

394 Veraart, A.J., de Klein, J.J.M., and Scheffer, M., 2011. Warming Can Boost Denitrification
395 Disproportionately Due to Altered Oxygen Dynamics. *Plos One* 6(3), e18508.
396 <https://doi.org/10.1371/journal.pone.0018508>.

397 Wang, X.J., Ye, C.S., Zhang, Z.J., Guo, Y., Yang, R.L., Chen, S.H., 2018. Effects of temperature shock
398 on N₂O emissions from denitrifying activated sludge and associated active bacteria. *Bioresource*
399 *Technol.* 249, 605–611. <https://doi.org/10.1016/j.biortech.2017.10.070>.

400 Wang, Y.T., Zhang, T.Q., Zhao, Y.C., Ciborowski, J.J.H., Zhao, Y.M., O'Halloran, I.P., Qi, Z.M., Tan,
401 C.S., 2021. Characterization of sedimentary phosphorus in Lake Erie and on-site quantification of
402 internal phosphorus loading. *Water Res.* 188, 116525. <https://doi.org/10.1016/j.watres.2020.116525>.

403 Wu, D., Well, R., Cardenas, L.M., Fuss, R., Lewicka-Szczebak, D., Koster, J.R., Bruggemann, N., Bol
404 R., 2019. Quantifying N₂O reduction to N₂ during denitrification in soils via isotopic mapping

405 approach: Model evaluation and uncertainty analysis. *Environ. Res.* 179, 108806.
406 <https://doi.org/10.1016/j.envres.2019.108806>.

407 Xiao, Y., Zheng, Y., Wu, S., Yang, Z.H., Zhao, F., 2015. Bacterial Community Structure of Autotrophic
408 Denitrification Biocathode by 454 Pyrosequencing of the 16S rRNA Gene. *Microb. Ecol.* 69(3),
409 492–499. <https://doi.org/10.1007/s00248-014-0492-4>.

410 Zhang, J.X., 2021. Spatial distribution of water quality and identification of pollution sources in Taihu
411 Lake Basin. *Jiangsu Sci. & Tec. Inform.* 38(10), 48–54. (In Chinese)

412 Zhang, X.M., Hua, X.F., Yue, X.P., 2017. Comparison of bacterial community characteristics between
413 complete and shortcut denitrification systems for quinoline degradation. *Appl. Microb. Biot.* 101(4),
414 1697–1707. <https://doi.org/10.1007/s00253-016-7949-y>.

415 Zhang, Y.L., Liu, M.L., Qin, B.Q., Feng, S., 2009a. Photochemical degradation of
416 chromophoric–dissolved organic matter exposed to simulated UV–B and natural solar radiation.
417 *Hydrobiologia* 627(1), 159–168. <https://doi.org/10.1007/s10750-009-9722-z>.

418 Zhang, Y.L., van Dijk, M.A., Liu, M.L., Zhu, G.W., Qin, B.Q., 2009b. The contribution of phytoplankton
419 degradation to chromophoric dissolved organic matter (CDOM) in eutrophic shallow lakes: Field
420 and experimental evidence. *Water Res.* 43(18), 4685–4697.
421 <https://doi.org/10.1016/j.watres.2009.07.024>.

422 Zhao, L.L., Zhu, M.Y., Feng, L.Q., Liu, X.H., Zhu, G.W., Chen, Y.F., Qin, B.Q., 2011. Stratification and
423 its driving factors of water physicochemical variables in large, shallow Lake Taihu. *J. Lake Sci.*
424 23(04), 649–656. (In Chinese)